Mon. Not. R. astr. Soc., (1986) **218,** 223–246

The geometry and distance of the Magellanic Clouds from Cepheid variables

John A. R. Caldwell★ and Iain M. Coulson *South African Astronomical Observatory, PO Box 9, Observatory 7935, South Africa*

Accepted 1985 July 25. Received 1985 July 4; in original form 1985 February 21

Summary. Period, luminosity and colour data on LMC and SMC Cepheids are analysed. A geometrical model for the LMC and the SMC is presented based on the Cepheids. The distance modulus of each Cloud is redetermined and its dependence upon the assumed abundance deficiency in the Clouds is made explicit. New, independent abundances are inferred based on the Cepheids alone, and are found to agree well with the known H II region abundance deficiencies. The luminosity laws in both galaxies, suitably corrected for abundance, are mutually consistent, enabling a 'universal' PLC and PL relation to be obtained which incorporates all the photoelectric data. Finally, it is argued that the 21 cm data of Mathewson & Ford are consistent with our view of the SMC as a two-armed galaxy, showing its central bar to us edge on, with a mass of material pulled out of its centre towards the SW seen in projection against the far arm. That the SMC consists of two separated fragments over much of its angular extent seems less plausible.

1 Introduction

Caldwell & Coulson (1984, CC1) have published extensive new $BVRI_C$ photometry of SMC Cepheids and have obtained additional LMC Cepheid photometry (Caldwell, Coulson, Spencer Jones & Feast, in preparation, CCSF) supplemental to that in Martin, Warren & Feast (1979, MWF). Caldwell & Coulson (1985, CC2) determined *BVI* reddenings for 48 SMC Cepheids and redetermined reddenings for 29 LMC Cepheids, using an intrinsic Cepheid colour locus corrected for metal deficiency. Excluding the dusty central region of each Cloud delineated by the dark nebulae, a mean $E(B-V)$ of 0.074 mag was found in the LMC and 0.054 mag in the SMC, with a small observed dispersion, 0.037 and 0.029 mag, respectively.

The present work uses the photoelectric results assembled for 73 LMC and 63 SMC Cepheids to obtain solutions for the PL, PC and PLC relations in the Clouds, and the Clouds' geometry and distance. Standard metal deficiency factors of $D_{\rm LMC}=1.4$ and $D_{\rm SMC}=4.0$ are assumed (CC2)

★Present address: Mt Wilson and Las Campanas Observatory, Carnegie Institution of Washington, 813 Santa Barbara St, Pasadena, CA 91101, USA.

based on spectrophotometric H II region abundances but in fact the Cepheid data allow an independent metallicity determination which agrees roughly with these values. 'Universal' Cepheid PL and PLC laws are obtained and their possible advantages and disadvantages pointed out. The PLC is confirmed to be an extremely useful distance indicator, contrary to recent assertions.

2 Period, luminosity, colour and Cloud geometry

Solutions have been obtained for the Cepheid PL, PC and PLC relations in the Clouds, taking into account that each Cloud may have a depth in the line-of-sight caused by inclination to the plane of the sky. As necessary input, the Cepheid period and angular position are straightforward, but the dereddened colour and magnitude require a value for $E(B-V)$. Thus we present in general two solutions: an 'individual reddenings' (IR) solution restricted to those Cepheids for which an individually measured reddening is available, and a 'statistical reddenings' (SR) solution. The latter assigns to all Cepheids away from the dusty core region of each Cloud the average $E(B-V)$ of all the individual reddening determinations, *unless* a given Cepheid reddening has been measured to be at least 2σ different from this value, in which case the measured reddening is adopted. The SR solution is motivated by the inference of a small intrinsic reddening dispersion among the Cepheids in each Cloud, suggesting the possibility of using the

Table 1. Numerical results from LMC solutions ($D=1.4$y).

Quantity	Solution 1		Solution 2	
N(SR)	73	(±)	19	(±)
A(PL)	−2.69	0.07		
B(PL)	17.05	0.09		
σ(PL)	0.23	0.02		
α(ML)	−3.51	0.09	−4.14	0.42
β(ML)	2.13	0.19	3.96	0.70
γ(ML)	16.48	0.06	15.71	0.15
σv(ML)	0.095		–	
α(LS)	−3.48	0.07	−3.68	0.13
β(LS)	2.04	0.15	2.67	0.31
γ(LS)	16.50	0.06	16.20	0.15
σ(LS)	0.121	0.010	0.089	0.014
GRAD (m/o)	0.0207	0.0050	0.0207	Fixed
INCL (°)	28.6	5.9	28.6	Fixed
P.A. (°)	232.4	7.7	232.4	Fixed
N(IR)	26		19	
A(PL)	−2.91	0.15		
B(PL)	17.42	0.23		
σ(PL)	0.22	0.03		
α(ML)	−3.80	0.13	−3.89	0.28
β(ML)	2.14	0.24	3.28	0.51
γ(ML)	16.86	0.11	15.96	0.14
σv(ML)	0.069		–	
α(LS)	−3.75	0.11	−3.61	0.12
β(LS)	2.01	0.21	2.48	0.29
γ(LS)	16.89	0.11	16.27	0.14
σ(LS)	0.100	0.014	0.088	0.014

Solution 1 uses $\langle V\rangle_0$ and $\underline{\langle B\rangle-\langle V\rangle_0}$ as magnitude and colour.
Solution 2 uses $\langle V\rangle_0$ and $\overline{V-I_0}$.

large number of Cepheids with satisfactory *BV* data but lacking *I*, and therefore lacking an individually measured reddening.

Table 1 gives numerical results from the PL and PLC solutions in the LMC, using statistical reddenings (top) and individual reddenings (bottom). Periods, colours, and magnitudes are from Martin & Warren (1979), MWF and CCSF. Reddenings are from CC2. Angular positions come from the *Radcliffe Observatory Memorandum No. 1* (1961) or sources cited in Hodge & Wright (1967). The first source enabled an approximate value of $\overline{V-I}$ to be obtained for 20 LMC Cepheids by curve fitting (unpublished). The quantities given in the Table are: N, the number of Cepheids in the solution; A, B and σ, the coefficients and standard deviation of the PL law

$$V^\circ = A \log P + B;$$

α, β, γ and σ, the coefficients and standard deviation of the PLC law

$$V^\circ = \alpha \log P + \beta(\text{colour})^\circ + \gamma;$$

GRAD and INCL, the inclination expressed in mag deg^{-1} and in deg; and PA, the position angle of the distance gradient direction (i.e. 90° from the line of nodes). LS refers to a standard multilinear least-squares solution for the PLC which assumes all error to be in V°, whereas ML refers to a maximum-likelihood solution which allows for errors in the colours and in the reddenings being non-negligible (Appendix A). The nominal centre of coordinates is that of the centre of the bar, $5^{\mathrm{h}}24^{\mathrm{m}}$ $-69^\circ.8$ (1950) (de Vaucouleurs & Freeman 1972).

The inclination was found iteratively by solving the maximum-likelihood PLC in $\langle V\rangle^\circ$ and $\langle B\rangle - \langle V\rangle^\circ$ assuming statistical reddenings, fitting the angular residuals $\delta\langle V\rangle^\circ$ in two dimensions by an inclined plane, re-solving the PLC(ML, SR) w.r.t. this plane, and so on. The PLC solution in $\overline{V-I}_0$ is extremely uncertain because of few points and therefore the geometry from the $\langle B\rangle - \langle V\rangle^\circ$ PLC solution was simply adopted.

In Table 1 the relatively small number of LMC Cepheids with individually determined reddenings available (26) explains the larger uncertainties on these solutions. There is an urgent need for more high accuracy *BVI* photometry of fainter LMC Cepheids.

Table 2 gives numerical results from the PL and PLC solutions in the SMC, using statistical reddenings (top) and individual reddenings (bottom). Periods, colours, magnitudes and angular positions are from CC1, CC2 and *Radcliffe Observatory Memorandum No. 1* (1961) or sources cited in Hodge & Wright (1977). The tabulated parameters are as described for the LMC, but for the addition of a third solution using the magnitude mean $\overline{B-V}_0$ as the colour instead of the difference of the intensity means $\langle B\rangle - \langle V\rangle^\circ$, since accurate $\overline{B-V}_0$s are available for all the SMC Cepheid sample. The nominal centre of coordinates is again that of the centre of the bar, $0^{\mathrm{h}}51^{\mathrm{m}}$ $-73^\circ.1$ (1950) (de Vaucouleurs & Freeman 1972). The inclination for each of the three solutions in Table 2 was found iteratively by solving the PLC(ML, SR) in the respective colour, fitting the angular residuals by an inclined plane and so on.

Numerical results for the observational PC relations in both Clouds and the Galaxy are given in Table 3. The Cloud data are from the sources already cited, whereas the Galactic data are from Schaltenbrand & Tammann (1971), Dean, Warren & Cousins (1978) and recent supplemental colours and reddenings from SAAO (Coulson, Caldwell & Gieren 1985a, b; Coulson & Caldwell 1985). The parameters tabulated are analogous to the preceding tables, except for referring to the PC law:

$$(\text{colour})^\circ = A \log P + B.$$

The colours predicted in each galaxy at a fiducial $\log P = 1.0$ are compared at the bottom of Table 3 and discussed later.

The above results are illustrated in plots 1–9. Figs 1 and 2 show the PL relation determined in

Table 2. Numerical results from SMC solutions (D=4y).

Quantity	Solution 1	(±)	Solution 2	(±)	Solution 3	(±)
N(SR)	63		63		43	
A(PL)	−2.88	0.11	−2.86	0.11		
B(PL)	17.72	0.15	17.69	0.15		
σ(PL)	0.26	0.02	0.26	0.02		
α(ML)	−3.67	0.10	−3.72	0.09	−3.79	0.10
β(ML)	2.28	0.19	2.34	0.19	3.86	0.31
γ(ML)	17.09	0.09	17.23	0.09	15.88	0.15
σv(ML)	0.129		0.127		0.097	
α(LS)	−3.68	0.09	−3.71	0.09	−3.71	0.09
β(LS)	2.30	0.18	2.30	0.17	3.57	0.25
γ(LS)	17.09	0.09	17.23	0.09	16.01	0.15
σ(LS)	0.134	0.012	0.136	0.012	0.112	0.012
GRAD (m/o)	0.0877	0.0108	0.0970	0.0137	0.1224	0.0168
INCL (°)	66.6	2.6	68.7	2.7	72.8	2.2
P.A. (°)	248.3	2.3	234.6	3.6	233.1	3.5
N(IR)	44		44		43	
A(PL)	−2.99	0.16	−2.95	0.16		
B(PL)	17.91	0.24	17.84	0.24		
σ(PL)	0.28	0.03	0.28	0.03		
α(ML)	−3.74	0.09	−3.76	0.09	−3.82	0.12
β(ML)	2.36	0.18	2.43	0.17	3.96	0.33
γ(ML)	17.12	0.10	17.20	0.09	15.85	0.15
σv(ML)	0.103		0.100		0.098	
α(LS)	−3.75	0.09	−3.76	0.09	−3.72	0.09
β(LS)	2.40	0.17	2.44	0.16	3.56	0.25
γ(LS)	17.11	0.10	17.20	0.09	16.04	0.15
σ(LS)	0.109	0.012	0.110	0.012	0.114	0.012

Solution 1 uses $\langle V\rangle_0$ and $\overline{B-V}^\circ$ as magnitude and colour.
Solution 2 uses $\langle V\rangle_0$ and $\langle B\rangle - \langle V\rangle_0$.
Solution 3 uses $\langle V\rangle_0$ and $\overline{V-I}^\circ$.

Table 3. Numerical results for period–colour relations.

Solution	GAL $\langle B\rangle-\langle V\rangle_0$	LMC $\langle B\rangle-\langle V\rangle_0$	SMC $\langle B\rangle-\langle V\rangle_0$	GAL $\overline{(B-V)}_0$	SMC $\overline{(B-V)}_0$	GAL $\overline{(V-I)}_0$	LMC $\overline{(V-I)}_0$	SMC $\overline{(V-I)}_0$
N(SR)		73	64		64		19	44
A(PC)		0.378	0.375		0.375		0.361	0.230
±		0.031	0.041		0.042		0.056	0.035
B(PC)		0.277	0.187		0.234		0.374	0.488
±		0.038	0.058		0.058		0.073	0.051
σ		0.097	0.100		0.097		0.070	0.069
N(IR)	108	26	45	108	45	82	19	44
A(PC)	0.412	0.419	0.358	0.461	0.341	0.292	0.318	0.227
±	0.023	0.066	0.057	0.023	0.055	0.022	0.054	0.038
B(PC)	0.310	0.259	0.222	0.297	0.296	0.443	0.433	0.498
±	0.022	0.096	0.087	0.022	0.083	0.022	0.074	0.057
σ	0.070	0.099	0.107	0.070	0.101	0.064	0.072	0.069
Colour at		0.655	0.562		0.609		0.735	0.718
Log P=1.0		±0.013	±0.019		±0.020		±0.022	±0.019
	0.722	0.678	0.580	0.758	0.637	0.735	0.751	0.725
	0.008	±0.035	±0.032	±0.008	±0.031	±0.008	±0.025	±0.019
Colour		−0.064	−0.155		−0.141		0.007	−0 013
Difference		±0.016	±0.024		±0.025		±0.025	±0.021

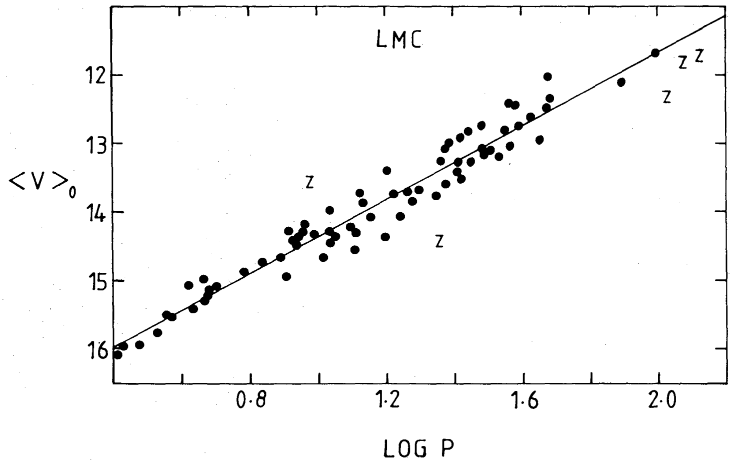

Figure 1. The period–luminosity relation in the LMC, excluding Cepheids marked as Z.

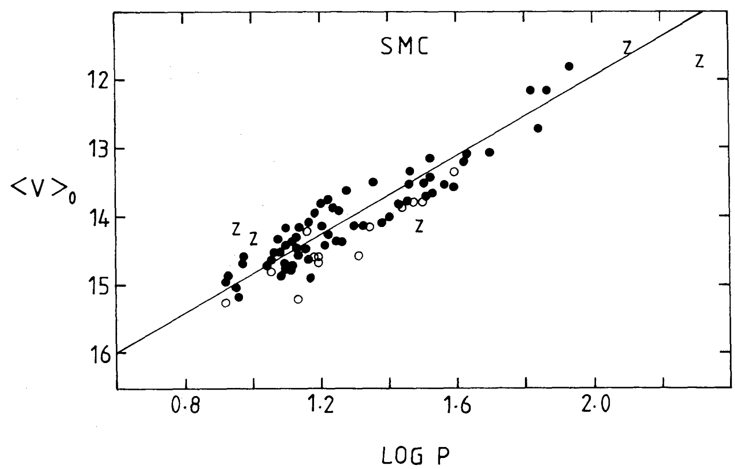

Figure 2. The period–luminosity relation in the SMC, excluding Cepheids marked as Z or open circles. The latter have unknown reddening and are located in the central dusty core. They would be underluminous if their reddening were the same as the measured average for the rest of the Cepheids, as assumed for this plot.

the LMC and SMC, respectively, assuming statistical reddenings. Filled circles are points included in the solution, open circles are points excluded from the solution corresponding to Cepheids lacking individual reddenings but lying in the high extinction central core of the SMC, and zs are points excluded from the solutions for other reasons (Appendix A). Averaged over different solutions, the apparent dispersions of the Cloud PL relations are 0.23 and 0.27 mag, respectively, ±10 per cent. Rather little of this spread is likely to be due to observational error and residual line-of-sight scatter (after having corrected for Cloud inclination). We estimate that σ(PL) would be 0.19 mag in the LMC and 0.23 mag in the SMC in the absence of such effects. The slope in the LMC is slightly (1.5σ) smaller due to what appears to be a concentration of Cepheids

Table 4. Period–colour strip widths (±).

	$\langle B\rangle - \langle V\rangle_0$	$\overline{B-V_0}$	$\overline{V-I_0}$
Galaxy	0.24 mag (0.02)	0.24 mag (0.02)	0.22 mag (0.02)
LMC	0.34 mag (0.03)		0.24 mag (0.02)
SMC	0.35 mag (0.03)	0.34 mag (0.03)	0.24 mag (0.03)

on the left of the instability strip at log $P<1.0$. It is also smaller (2.1σ) than that found for the Galactic calibrators in Table 5, -2.96 ± 0.11.

Figs 3–5 show PLC relations projected on to a plane of colour equals nought. The relations based upon $\langle B\rangle - \langle V\rangle^{\circ}$ and $\overline{V-I_0}$ in the LMC have apparent dispersions 0.12 and 0.09 mag, respectively, ±0.01 mag. Of course, the photometry itself is much better than this but the observed scatter in the LMC can none the less be roughly accounted for by the propagation of the estimated observational errors ($\sigma^2=\sigma_V^2+\beta^2\sigma_C^2+(R-\beta)^2\sigma_E^2$, see Appendix A). The PLC relation based on $\overline{B-V_0}$ or $\langle B\rangle - \langle V\rangle^{\circ}$ and $\overline{V-I_0}$ in the SMC have apparent dispersions 0.14 and 0.11 mag, respectively, ±0.01 mag, significantly larger than expected from compounding of the (smaller) estimated average observational errors of the SMC data. This suggests additional (non-planar) line-of-sight structure, in which case the PLC in both Clouds would be consistent with being intrinsically exact, as discussed later.

Figs 6 and 7 illustrate the angular regression of the magnitude residuals using a

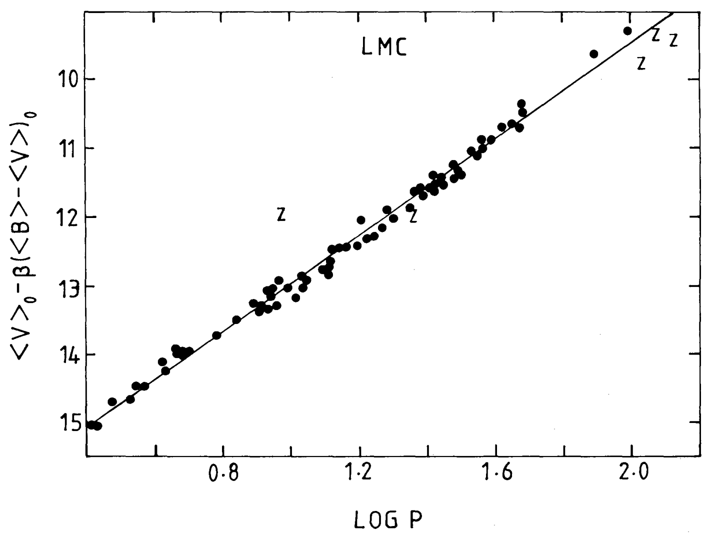

Figure 3. The projected period–luminosity–($\langle B\rangle - \langle V\rangle_0$) colour relation in the LMC, which has negligible intrinsic scatter in view of the observational errors.

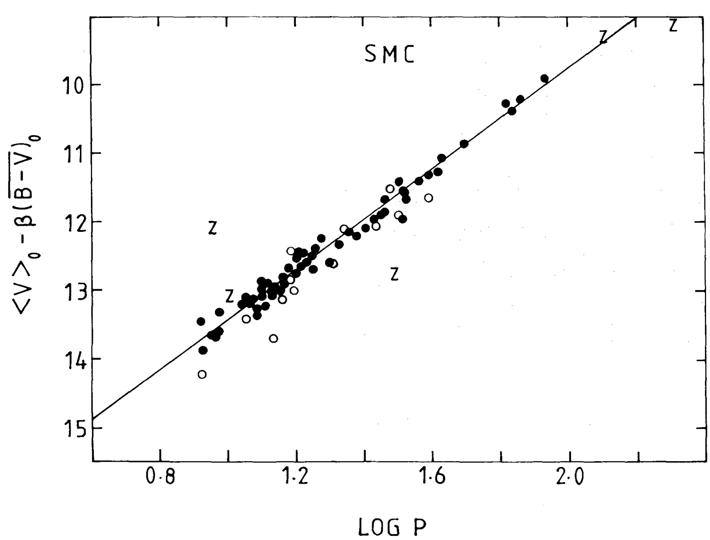

Figure 4. The projected period–luminosity–($\overline{B-V^{\circ}}$) colour relation in the SMC, which has negligible intrinsic scatter in view of the observational errors and likely line-of-sight spread in the SMC.

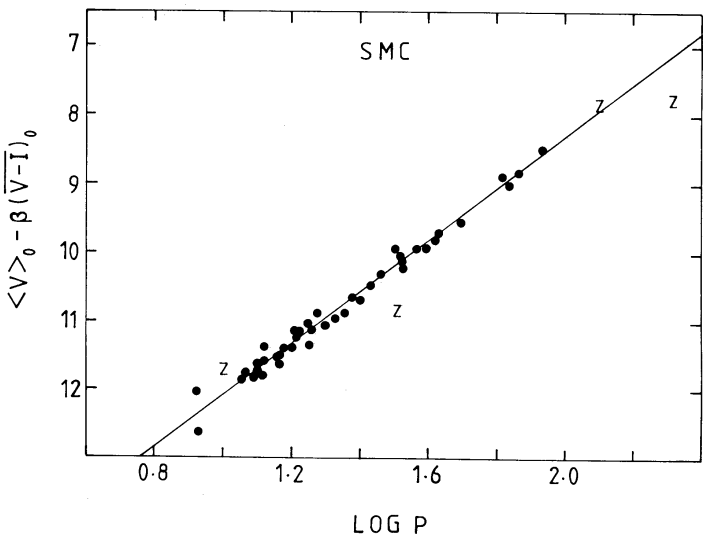

Figure 5. As Fig. 4 but for $\overline{V-I^\circ}$.

PLC(ML, SR, $\langle B\rangle-\langle V\rangle^\circ$) solution in the LMC and a PLC(ML, SR, $\overline{B-V_0}$) solution in the SMC. These two solutions are considered to show the most accurate currently available picture of the line-of-sight dimension of the two Clouds and give results which are fairly similar to those from the other possible solutions (least-squares or individual reddenings or other colours). The

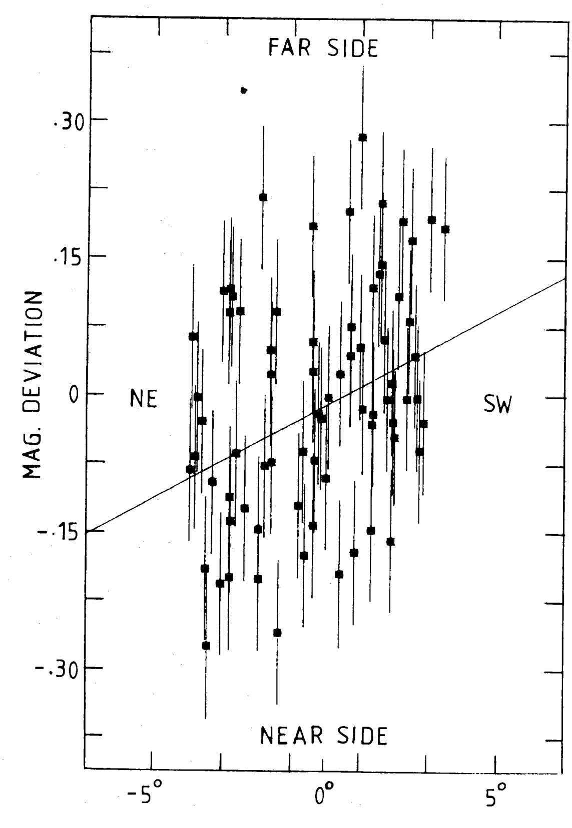

Figure 6. The regression of PLC magnitude residuals versus angle across the LMC along the direction of the maximum distance gradient, showing in effect the line-of-sight structure of the Cloud. The horizontal ticks (2×1°) correspond to the same linear distance as the vertical ticks (2×0.0389 mag).

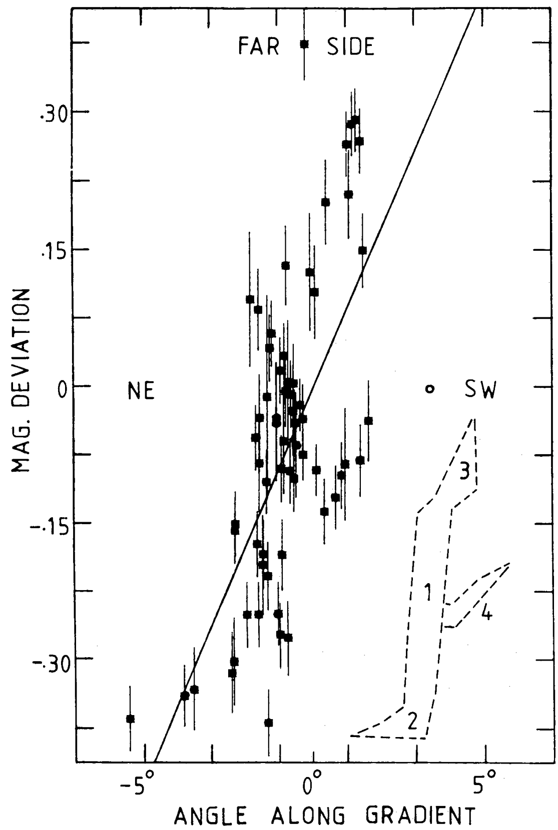

Figure 7. As Fig. 6 but for SMC. The dashed outline sketches in miniature (1) the main bar (2) the near arm (3) the far arm and (4) the material extending from the centre to the SW and overlapping in projection against the far arm.

abscissa is angle in degrees and the ordinate is magnitude in units of 0.0389 mag, such that the x- and y-axes correspond to equivalent scales of linear distance. The angle is measured positively from the coordinate centre in the direction of the maximum distance gradient, which points roughly SW in each case. In effect, Figs 6 and 7 show the Clouds as they might appear viewed from along their line of nodes in the plane of the sky. The filled circles in each plot show Cepheids in the solution. The error bars (Appendix A) appear large because of the large magnification of the y-coordinate to match the x-coordinate in linear scale, and especially in the case of the LMC because of the method of data analysis. One Cepheid preceding the SMC (R Hyi=HV 6320) has excellent data but was excluded from the solution for being too inconsistent with a planar approximation, although it is no doubt a member of that galaxy (*cf.* open circle in Fig. 7).

Despite the apparent 'thickness' of the LMC Cepheid distribution, error analysis indicates that the spread is less than 2σ different from zero, if all estimated errors are uncertain by 20 per cent. Our model for the LMC is thus an inclined plane of insignificant thickness, tipped by $29\pm6°$ with the closest part at PA $52\pm8°$. The SMC appears to consist of a 5-to-1 central bar seen edge-on, a near arm (NE) and far arm (SW), and a mass of material pulled out of the centre of that galaxy, perhaps by the LMC, and seen in projection in front of the far arm in the SW (*cf.* sketch in Fig. 7). A model of a single inclined plane is obviously inadequate and error analysis shows that the residual line-of-sight scatter about the inclined-planar solution is very significantly different from zero. The size and direction of the maximum distance gradient is thus not a very meaningful quantity. An average of the results from the three solutions gives an inclination of $70\pm3°$ with the closest part at PA $58\pm10°$.

The line-of-sight scatter inferred for the SMC Cepheids (0.10–0.13 mag, depending on the model) is reasonable given that a planar model looks barely adequate to describe the SMC. The line-of-sight scatter for the LMC Cepheids is small, perhaps negligible. This empirically refutes Stift's (1982) assertion that scatter caused by mass loss and multiple instability strip crossings is likely to be comparable to the instability strip width, rendering 'the very concept of a PLC relation meaningless'.

Figs 8 and 9 show an aerial view of the Cepheid magnitude residuals on the sky, corresponding

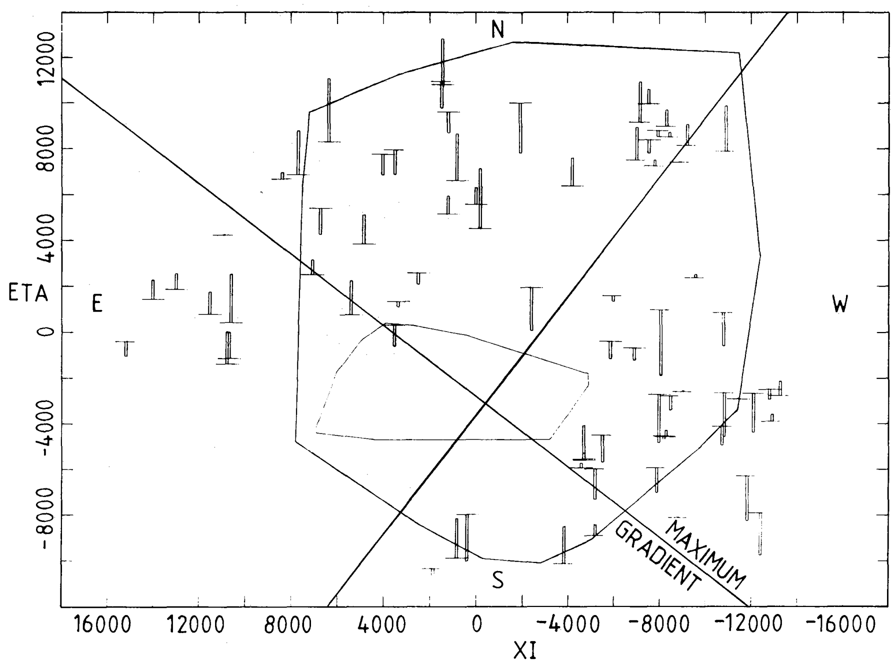

Figure 8. Aerial view of LMC Cepheid magnitude residuals in Wesselink (1959) coordinates (in arcsec). Vertical bars of length ±1 tick denote magnitude residuals w.r.t. the coordinate centre of ±0.2 mag. The outer perimeter sketches the limit of the Cloud bright nebulae, and the inner perimeter the limit of the high opacity dark nebulae.

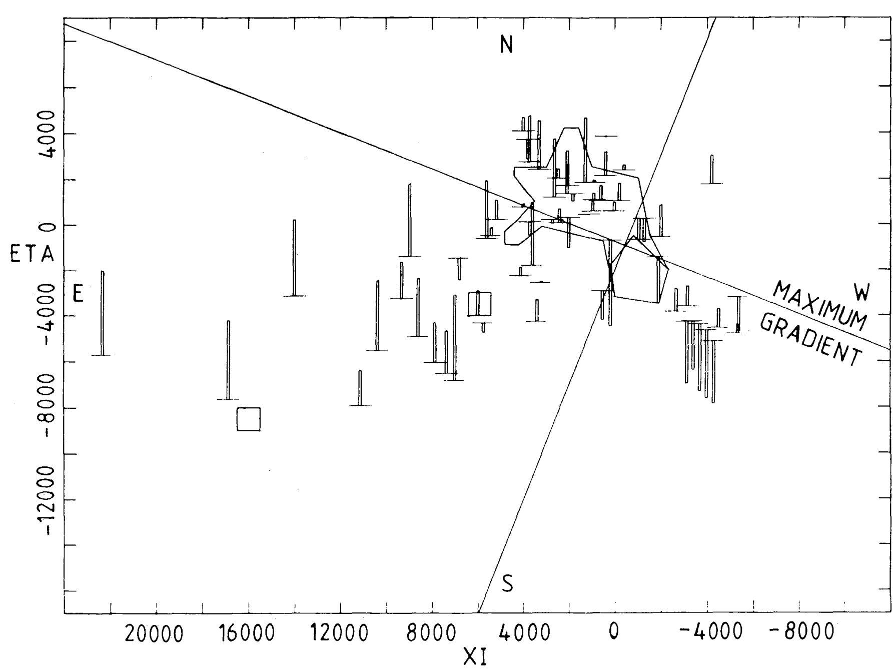

Figure 9. As Fig. 8 but for SMC. The inner perimeter is the pentagon SW of the centre, and the 'wing' regions K1 and K2 are the two squares plotted right to left.

to the same solutions as in Figs 6 and 7. The outer and inner perimeters sketched for each Cloud indicate the outlines of the concentrations of bright nebulae (Davies, Elliott & Meaburn 1976) and dark nebulae (Hodge 1972, 1974). The straight lines show the direction of the maximum distance gradient, the line of nodes, and the position of the coordinate centre. The SMC 'wing' regions K1 and K2 (de Vaucouleurs & Freeman 1972) are shown as two squares. Cepheids in the solution are denoted by short horizontal lines. A bar of length one unit above or below the horizontal line indicates a magnitude residual for that Cepheid of −0.2 or +0.2 mag, respectively.

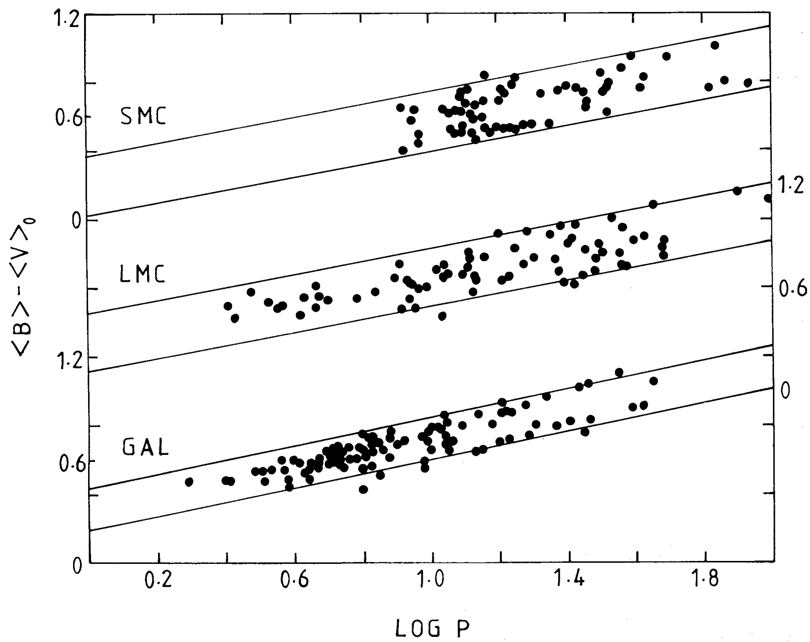

Figure 10. The period–($\langle B\rangle$–$\langle V\rangle_0$) colour relation in the SMC, LMC, and the Galaxy. The strip edges correspond to a width of $\sqrt{12}\sigma$, which assumes a statistically uniformly filled strip.

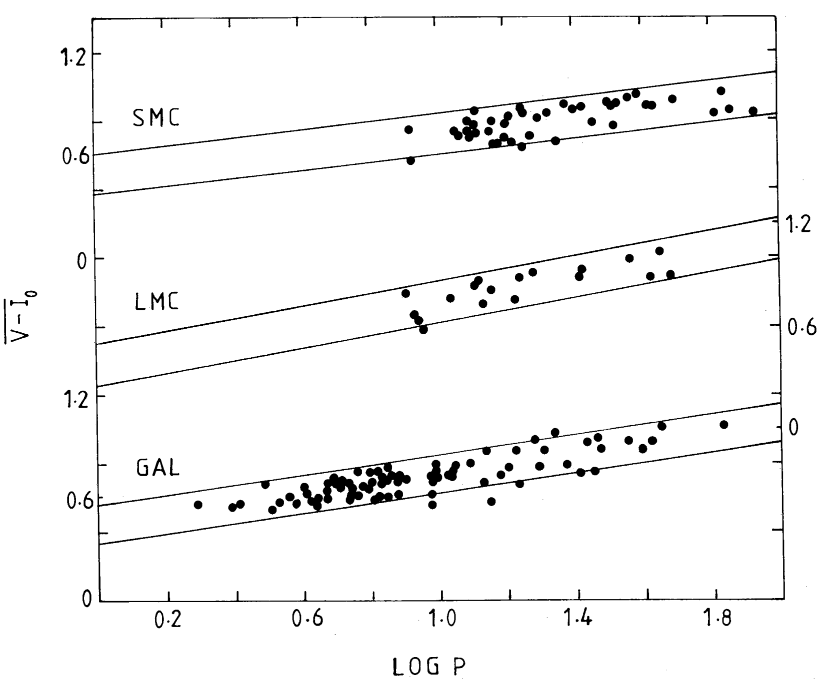

Figure 11. As Fig. 10 but for $\overline{V-I_0}$.

The large distance spread of the SMC is especially obvious in the last figure. It is perhaps interesting to note that if the Cloud Cepheids had the same distance dispersion in the line-of-sight as they show angular dispersion on the sky, then the dispersion of Cepheid magnitudes would be 0.10 mag in the LMC and 0.07 mag in the SMC.

Expressed as Wesselink coordinates (Wesselink 1959) the inclination of the LMC is found to be $\nabla\xi=-0.0164$, $\nabla\eta=-0.0126$ mag per deg from centre $(-418, -3114)$ and of the SMC is $\nabla\xi=-0.0861$, $\nabla\eta=-0.0540$ mag per deg from centre $(-422, -929)$. Thus the LMC plane projects to 0.45 mag behind the LMC centre at the line-of-sight to the SMC, and the SMC plane projects to 1.22 mag in front of the SMC centre at the line-of-sight to the LMC, ignoring the non-linearity of the magnitude–distance conversion. From the differential distance moduli obtained in the next section it will be seen that the SMC may well be situated in the plane of the LMC but not vice versa.

Figs 10 and 11 show the PC relations in the SMC, LMC and the Galaxy, respectively, again assuming statistical reddenings in the Clouds. The strip edges shown are calculated by assuming that the strip width must equal $\sqrt{12}\sigma$ in the idealization of a uniformly filled strip parent distribution. The lack of $V-I$ data in the LMC and of data on faint Cloud Cepheids in general is apparent. There appear to be no significant differences of slope but the width of the PC strip in $B-V$ is definitely larger in the Clouds than in the Galaxy, while the $V-I$ strip width is the same (*cf.* Table 4). Corrected for observational error, the $B-V$ strip widths are ~0.32 mag and the $V-I$ widths ~0.21 mag in the Clouds. The apparently real increase in $B-V$ strip width in the Clouds compared to the Galaxy may be due to the selection effect excluding short-period Cloud Cepheids, coupled with an empirical narrowing of the PC($B-V$) relation towards shorter periods.

3 Modulus and metallicity

The determination of the distance moduli to the Clouds (viz. at their centres of coordinates) is a problem whose solution is moderately sensitive to the abundance deficiency inferred to exist there. Dennefeld & Stasinska (1983), Dufour (1984), McGregor & Hyland (1984) and Feast (1984, 1985) have recently found values for the metal deficiency factor $D=Zo/Z$ ranging from 1.4–1.8 in the LMC and 3–4.2 in the SMC. We adopt Feast's $D_{\rm LMC}=1.4$ and $D_{\rm SMC}=4.0$ for our standard models but give alternative results for $D_{\rm LMC}=1$–2 and $D_{\rm SMC}=2$–8 for comparison.

Lequeux *et al.* (1979) showed that He is deficient proportionally to the metal deficiency, and we adopt their coefficient $\Delta Y=2.8\,\Delta Z$, where $\Delta()=()-()^{\circ}$. Thus we choose $D_{\rm LMC}=1.4$y and $D_{\rm SMC}=4$y, where 'y' symbolizes that He is also considered deficient in the quoted proportion.

Much consideration has been given to the calibrating Cepheids recently (Balona & Shobbrook 1984; Caldwell 1983; Coulson & Caldwell 1985; Dean, in preparation; Fernie & McGonegal 1983; Pel 1985; Stothers 1983; Turner 1984; Turner & Evans 1984; Walker 1985). We adopt in Table 5 a fairly uncritical average of all the material available at this time, scaled to a Pleiades distance modulus of $(m-M)_{\rm M45}=5.57$ mag (Pel 1985). The ensemble of material suffices to determine a modulus to ±0.04–0.05 mag (internal s.e.m.) and corresponds to a zeropoint of −2.40 in terms of the PLC law obtained by MWF.

One best calculates a modulus for each Cloud by calibrating the PL or PLC relation determined in that Cloud by means of the Galactic Cepheids of approximately known distance. Since the Galactic Cepheids according to theory (Appendix B) do not obey the same PLC as the Cloud Cepheids (different Y and Z), one must first correct the coefficients α, β and γ for the PLC composition-dependence. Failure to do so would incur an error in distance modulus amounting to +0.14 ($B-V$ PLC) or +0.07 ($V-I$ PLC) in the LMC and amounting to +0.51 ($B-V$ PLC) or +0.22 ($V-I$ PLC) in the SMC. Table 6 gives the distance moduli calculated assuming three values for the LMC metallicity and three for the SMC, which roughly bracket the maximum ranges of

Table 5. Values used for calibrators $\{(m-M)_{\mathrm{M45}}=5.57\}$.

Calibrator	M_V°	$\langle B\rangle-\langle V\rangle^\circ$	$\overline{B-V}^\circ -(\langle B\rangle-\langle V\rangle)^\circ$	$\overline{V-I}^\circ$	Weight
SU Cas	−2.12	0.50	0.01	0.58	2
EV Sct	−2.80	0.52	0.01	0.67	4
α UMi	−3.21	0.39	0.00	0.65	1
CEb Cas	−3.22	0.61	0.02	–	4(0)
CF Cas	−3.10	0.70	0.02	0.77	4
HD 144972	−3.06	0.67	0.01	0.69	1
CEa Cas	−3.30	0.69	0.02	–	4(0)
UY Per	−3.53	0.65	0.04	0.69	3
CV Mon	−3.48	0.58	0.02	0.69	4
V Cen	−3.35	0.56	0.03	0.62	2
VY Per	−3.90	0.66	0.03	0.71	2
CS Vel	−2.66	0.62	0.03	0.68	0
V367Sct	−3.67	0.57	0.01	0.74	3
U Sgr	−3.83	0.69	0.03	0.71	4
DL Cas	−3.85	0.70	0.02	0.74	4
S Nor	−4.03	0.74	0.02	0.78	4
TW Nor	−3.80	0.79	0.04	0.73	4
VX Per	−4.26	0.73	0.02	0.73	2
CPD-537400p	−3.97	0.81	0.00	0.79	1
SZ Cas	−4.74	0.67	0.01	0.73	2
VY Car	−5.00	0.92	0.06	0.87	3
RU Sct	−5.32	0.74	0.06	0.78	3
RZ Vel	−5.20	0.81	0.09	0.87	3
WZ Sgr	−4.74	0.94	0.06	0.98	2
SW Vel	−5.26	0.81	0.10	0.79	2
T Mon	−5.52	0.99	0.06	0.91	2
KQ Sco	−5.56	1.04	0.04	0.95	2
SV Vul	−6.08	1.02	0.07	0.97	2
GY Sge	−6.34	1.12	0.04	–	2(0)
S Vul	−6.90	1.12	0.03	0.99	3

Table 6. Effect of changed metallicity upon modulus and colours.

	LMC $D=1$	LMC 1.4y	LMC 2y	±	SMC $D=2$y	SMC 4y	SMC 8y	±
μ(ML)	18.72	18.60	18.49	0.06	19.12	18.93	18.82	0.07
$(\langle B\rangle-\langle V\rangle)$	18.81	18.70	18.59	0.06	19.12	18.94	18.84	0.07
μ(ML)					19.07	18.88	18.78	0.07
$(\overline{B-V})$					19.07	18.90	18.80	0.07
μ(ML)	18.85	18.75	18.64	0.10:	19.23	19.04	18.96	0.07
$(\overline{V-I})$	18.81	18.73	18.64	0.10:	19.22	19.05	18.95	0.07
μ(PL)	18.48	18.55	18.63	0.06	18.90	19.03	19.13	0.08
	18.62	18.71	18.79 ·	0.11	18.91	19.11	19.21	0.12
$\Delta(\langle B\rangle-\langle V\rangle)_0$	−0.086	−0.064	−0.044	0.017	−0.197	−0.155	−0.121	0.024
$\Delta\,\overline{B-V_0}$					−0.185	−0.141	−0.111	0.023
$\Delta\,\overline{V\text{-}I_0}$	−0.024	+0.007	+0.046	0.024	−0.079	−0.013	+0.031	0.021

Δ=Colour difference at log P=1.0 in sense Cloud–galaxy.

uncertainty of the Cloud abundances. The moduli are obtained from the maximum-likelihood PLC solutions using $\langle B\rangle-\langle V\rangle$, $\overline{B-V}$ and $\overline{V-I}$, and from the PL solution, taking into account that the Cepheid reddenings depend on the assumed metallicity. The two figures given one above the other show the statistical reddenings result above and the individual reddenings result below.

The error on the modulus includes both the internal error due to the calibrators' scatter and the effect of uncertainty in the luminosity law coefficients but not the uncertainty of the Pleiades modulus. Specifically, the effect of the calibrators' mean period and colour differing from those of the test objects establishing the luminosity law is rigorously included in the estimated errors. Stift's (1982) criticism of moduli obtained by the present method instead of by comparing 'mean magnitudes and colours at a standard period' appears to be based upon confusing σ(zeropoint) with σ(predicted magnitude at the period and colour of a calibrator).

The PLC moduli in Table 6 are a decreasing function of the assumed metal deficiency because of the PLC metal dependence. On the other hand the PL moduli are an increasing function of the assumed metal deficiency because of the blanketing and hence reddening dependence on metals. Given the contrary dependences, the PLC and PL together put a constraint on the plausible metal deficiency in each Cloud. Fig. 12 shows the mean and standard deviation of the moduli obtained (solid line and hatched boundaries) from the various luminosity laws, the exact weighting being unimportant. The weight of all available data favours $\mu_{\rm LMC}=18.65\pm0.07$ ($D_{\rm LMC}=1.4$y) and $\mu_{\rm SMC}=18.97\pm0.07$ ($D_{\rm SMC}=4$y). Somewhat better agreement between the various laws results if $D_{\rm LMC}\sim1.6$y and $D_{\rm SMC}\sim3.1$y ($\mu=18.63$ and 19.01 ± 0.06, respectively). For arbitrary ΔZ we obtain:

$$\mu_{\rm LMC}=18.696-6.630\,|\Delta Z|-317.0\,\Delta Z^2$$

$$\mu_{\rm SMC}=19.333-21.83\,|\Delta Z|-151.8\,\Delta Z^2.$$

If helium is assumed not to be deficient in the Clouds (i.e. $D_{\rm LMC}=1.4$ and $D_{\rm SMC}=4$, $\Delta Y=0$), then the PLC moduli are decreased by 0.034 and 0.078, respectively, while PL moduli are unchanged. The dotted lines in Fig. 12 illustrate the shift in the mean modulus if only Z but not Y is assumed to be deficient.

One might query these moduli on three grounds: the value used for $R\{=A_V/E(B-V)\}$, the sensitivity to choosing a maximum-likelihood rather than least-squares solution, and the theoretical possibility that the colour term β is not a constant with $\log P$ (Appendix B).

From Feast & Whitelock (1984), Nandy (1984) and Prevot *et al.* (1984) it is reasonable to take $R_{\rm MC}=R_{\rm GAL}$. Our model for R comes from Schmidt-Kaler (1982), yielding $R_{\rm avg}=3.52$ for the LMC and 3.50 for the SMC. Although $R_{\rm Ceph}\sim3.3$ is preferred by some, the effect of such a zeropoint shift in R on our solutions is negligible, $\Delta\mu=0.01$–0.02, with the effect on all other solution parameters similarly small.

For all models except the $V-I$ PLC in the LMC, which is very uncertain, the effect on the modulus of using the LS rather than the ML coefficients is negligible, -0.005 ± 0.01.

The possibility that the colour term, rather than being constant as generally assumed, increases moderately with $\log P$ is of more concern, since the Cloud Cepheids' larger mean $\log P$ relative to the Galactic calibrators could produce a bias in the modulus were this true. Solutions were obtained using the theoretical $\partial\beta/\partial(\log P)$ factors in Appendix B. The LMC PLC using $\langle B\rangle-\langle V\rangle$ and statistical reddenings gives the same modulus assuming $\partial\beta/\partial(\log P)\neq0$, for the reason that in this solution the test objects have almost as small a mean $\log P$ as the calibrators. For all other solutions the mean $\log P$ is 0.35–0.5 greater than that of the calibrators, resulting in moduli which are 0.05 ± 0.02 greater. Thus most of the PLC moduli obtained here *might* be $\sim$0.05 mag too small for ignoring a *possible* trend in β versus $\log P$.

Since an abundance deficiency factor must be adopted in order to get a definite prediction for

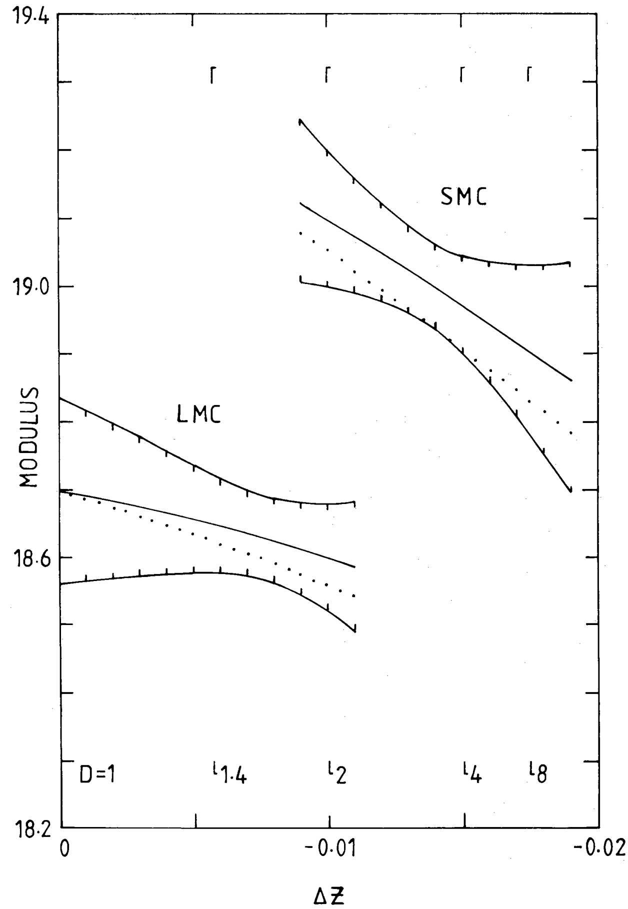

Figure 12. Mean and standard deviation (solid line and hatched boundaries) of the Cloud distance moduli inferred from the luminosity law solutions, as a function of the assumed Cloud metal deficiency, $\Delta Z = Z - Zo$ $(D = Zo/Z)$. The dotted line shows effect on the mean modulus if helium is assumed to be non-deficient.

the modulus from Fig. 12, it is of interest to note that the period–colour relations in the Clouds set a useful independent constraint on the metallicity. Consider the 'colour discrepancy':

$$\delta(\text{colour}) = (\text{col}_{\text{MC}} - \text{col}_{\text{GAL}})^{\text{OBSERVED}} - (\text{col}_{\text{MC}} - \text{col}_{\text{GAL}})^{\text{PREDICTED}},$$

where the possible colours are $B-V$ and $V-I$ and the evaluation is done at a fiducial $\log P = 1.0$ (the period–colour slopes appearing similar in all systems). The observed colour difference is given in the bottom of Table 3 for the standard metal deficiency factors and in the bottom of Table 6 for alternative metal deficiencies, which affect it through changed blanketing and hence reddening (see CC2). The predicted colour difference depends on metallicity in a different manner, as discussed below, allowing an optimal range of metallicity to be determined by the requirement $|\delta(\text{colour})| \leq \sigma_\delta$, where σ_δ is the standard error of δ.

Fig. 13 shows the colour discrepancy as a function of the assumed metallicity deficit. The top half shows $\delta(B-V)$, the bottom half $\delta(V-I)$, the left side the LMC, and the right side the SMC. The pair of solid lines in each quadrant enclose the band $|\delta| \leq \sigma_\delta$, if the Cloud colours are predicted to be bluer because of both decreased blanketing and higher temperature at fixed $\log P$, whereas the pair of dashed lines show $|\delta| \leq \sigma_\delta$, if the Cloud colours are bluer because of changed blanketing only. The latter assumption is less credible because one infers from Iben & Renzini (1984) that an ensemble of Cepheids in a metal-poor system will be hotter at fixed $\log P$ than an ensemble of metal-normal Cepheids by $\Delta \log T = -(4.2\,\Delta Z - 0.5\,\Delta Y)/3.45$. Considering the solid lines it is immediately clear that only a rather restricted range of metallicity produces agreement

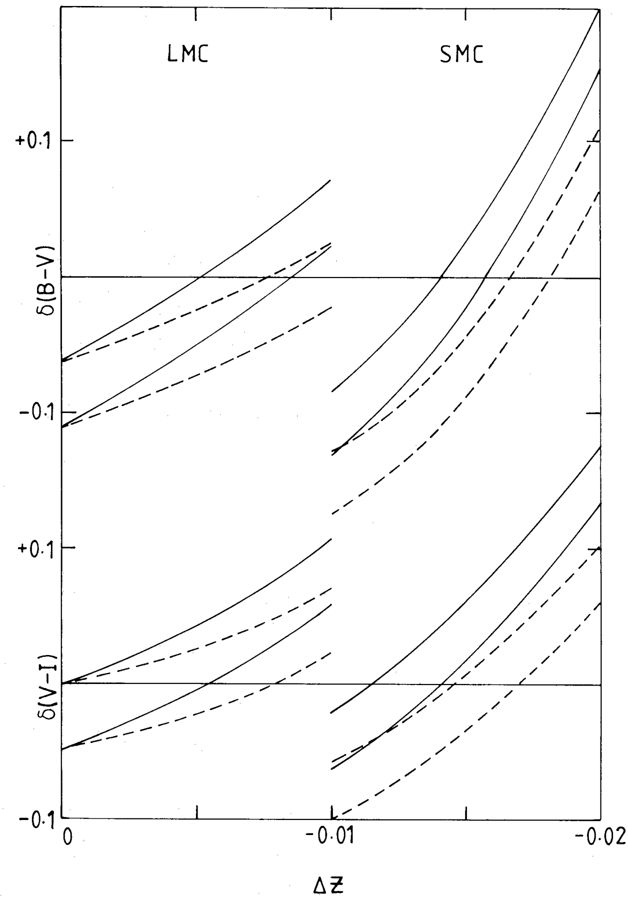

Figure 13. The 'colour discrepancy' between the observed and predicted mean colour at log $P=1.0$ in the LMC (left) and SMC (right), considering $B-V$ (top) and $V-I$ (bottom), as a function of the assumed Cloud metal deficiency. The pairs of lines (solid or dashed depending on assumptions, *cf.* text) show the $\pm 1\sigma$ bounds on the discrepancy, which will be consistent with zero for only a limited possible range of metal deficiency.

between the observed and predicted colour differences between the galaxies. Only $D_{\mathrm{LMC}}\sim 1.4$ and $D_{\mathrm{SMC}}\sim 3.4$ give mutual agreement between both the $B-V$ and $V-I$ criteria. One concludes from this and the PL–PLC interagreement discussed earlier that $D_{\mathrm{LMC}}\sim 1.4$–1.6 and $D_{\mathrm{SMC}}\sim 3.1$–3.4 are favoured by the Cepheid data on their own.

4 'Universal' PLC and PL laws

A universal PL and (metal-normal) PLC law can be obtained from a joint solution using up to 136 Cloud Cepheids to define the coefficients {scaled to $(m-M)_{\mathrm{M45}}=5.57$ mag}, and taking into account the different distance and metallicity of the Clouds and their inclinations. These luminosity laws can then be used to obtain distances to Cepheids in any galaxy, but for a metal-deficient Cepheid the PLC-law α, β and γ must of course first be adjusted (Appendix B).

From the statistical reddenings solutions we obtain for metal-normal Cepheids:

$$M_V^{\circ}=-3.53\log P+2.13\langle B\rangle-\langle V\rangle^{\circ}-2.25; \qquad n=136$$
$$(\mu_{\mathrm{LMC}}=18.62, \qquad \Delta\mu=0.30, \qquad \sigma_{Mv^{\circ}}\sim 0.01\text{–}0.03)$$

$$M_V^{\circ}=-3.52\log P+2.11\,\overline{B-V^{\circ}}-2.31; \qquad n=63$$
$$(\mu_{\mathrm{SMC}}=18.88, \qquad \sigma_{Mv^{\circ}}\sim 0.02\text{–}0.05)$$

$M_V^\circ = -3.66 \log P + 3.71\, \overline{V - I^\circ} - 3.39;$ $n=43$
($\mu_{\rm SMC} = 19.04$, $\sigma_{Mv^\circ} \sim 0.02$–$0.05$)

$M_V^\circ = -2.78 \log P - 1.41;$ $n=136$
($\mu_{\rm LMC} = 18.57$, $\Delta\mu = 0.42$, $\sigma_{Mv^\circ} \sim 0.21$),

where μ are the Cloud moduli inferred by the particular solution and σ_{Mv° gives the approximate error of a predicted absolute magnitude. For the PLC, σ_{Mv° is indicated as a range since the M_V° inferred will be most accurate for a Cepheid with the same log P and colour as the mean of the Cepheids used to establish the luminosity law and less accurate for increasingly different periods and colours as, e.g. those of the calibrating Cepheids. For the PL, σ_{Mv° is dominated by the intrinsic width of the instability strip in the PL plane.

These σ_{Mv° assume that the adopted magnitudes of the calibrators are consistent with $(m-M)_{\rm M45} = 5.57$ mag, but this assumption is uncertain by ± 0.04–0.05 mag and the figure 5.57 is itself uncertain by ± 0.08 (Pel 1985), so that the *true* absolute magnitude scale has an additional uncertainty of ~ 0.09 mag combined with the errors on the *relative* absolute magnitude scale as just discussed.

The luminosity laws just given, adjusted for metallicity in the case of the PLC (Appendix B), contain effectively all the magnitude-predictive information for Cepheid variables based upon photoelectric photometry. The PLC has the advantage of negligible intrinsic spread, according to our error analysis, but is dependent on models for the abundance dependence of the Cepheid mass–luminosity relation and colour–temperature–gravity relation. The PL has considerable intrinsic spread because of discarding the theoretically necessary third parameter, but is fortunately abundance-independent (except for the reddening correction). Thus in the case of a sufficiently large ensemble of Cepheids which (uniformly) fill in the strip, the PL can give as accurate a modulus as the PLC. However, for an individual Cepheid whose metallicity is not too uncertain, the PLC modulus is much to be preferred.

5 Comparison with Martin, Warren & Feast (1979)

This work is heavily indebted to the LMC Cepheid analysis of MWF and agrees with it in most essentials. One divergence is our finding the PLC colour term β to be in the range 2.1–2.2, whereas MWF obtained 2.7, both ± 10 per cent. Note that this has little repercussion on other matters such as the distance moduli, because any possible error in β is strongly coupled with and mostly compensated for by the error in α. The difference in β can be illustrated by five solutions: (1) least-squares in V° with the MWF data, (2) least-squares in C° with the MWF data, (3) maximum-likelihood with $\sigma_{v^\circ}/\sigma_{c^\circ} = 3/4$ with the MWF data (i.e. the solution espoused by MWF), (4) our approach with the MWF data, and (5) our approach with 'our' data, viz., the individual reddenings solution given in the lower half of Table 1.

Solution (1) has $\beta = 2.18 \pm 0.23$, a lower limit assuming all error in the magnitude. Solution (2) has $\beta = 2.75 \pm 0.27$, an upper limit assuming all error in the colour. Solution (3) assumes in effect $\sigma_{v^\circ} = 0.034$ mag and $\sigma_{c^\circ} = 0.046$ mag in absolute value, because MWF specify in their solution method only the ratio $\sigma_{c^\circ} : \sigma_{v^\circ}$ to be 4 : 3. Since $(\sigma_{v^\circ}/\sigma_{c^\circ} = 0.75) \ll (2.45 = \text{PL-width/PC-width})$, their solution allots almost all of the relative error to the colour axis rather than to the magnitude axis. Hence, there results $\beta = 2.70 \pm 0.27$, almost corresponding to the case of assuming least-squares in the colour.

Solution (4) still uses the MWF data but with several changes of approach: $\sigma_v = 0.025$ and $\sigma_c = 0.030$ are estimated from the internal s.e.m. of the MWF Table 2 data, $\sigma_{E(B-V)} \sim 0.023$ is estimated from CC2, and the inclination of the LMC is incorporated in the solution. A smaller colour term, $\beta = 2.21 \pm 0.26$ results for two main reasons. First σ_{c° no longer dominates the total spread, and secondly, $\sigma_{E(B-V)} \neq 0$ causes coupling of the magnitude and colour errors that tends to decrease β by of order 0.1. Lastly, solution (5) substitutes the new reddenings from CC2, updates the data on the three Cepheids in CCSF, removes two Cepheids used in MWF (HV 900, 909) due to lack of sufficient reddening measures, and adds two Cepheids (HV 5497, 2827) dropped by MWF. This is our adopted solution using individual reddenings (Table 1). with $\beta=2.14\pm0.24$.

6 Comparison with Mathewson & Ford (1984)

The quantitative analysis of the geometry of the Magellanic Clouds was pioneered by de Vaucouleurs (1955) (*cf.* de Vaucouleurs & Freeman 1972). Important recent discussions of this problem are given by Gascoigne & Shobbrook (1978), Ardeberg & Maurice (1979), de Vaucouleurs (1980), Azzopardi (1981a, b), Florsch, Marcout & Fleck (1981), McGee & Newton (1981), Bajaja & Loiseau (1982), Rohlfs *et al.* (1984), and the proceedings of *IAU Symposium 108*. For brevity we can here compare only with the important study by Mathewson & Ford (1984) in the last work cited. These authors provide a very illuminating view of the SMC in their fig. 4, which shows contours of H I emission along the major axis of the SMC as a function of velocity. Their figure is abstracted in Fig. 14 of this paper, and the PLC Cepheid distances from solution PLC(ML, SR, $\overline{B-V^{\circ}}$) are overlaid on the H I contours by projection of the Cepheids on to the H I strip map, and by an arbitrary vertical scaling choice ($-14\,\mathrm{km\,s^{-1}}$ per 0.1 mag) and shift. The correspondence is suggestive that the distance trend and velocity trend are highly correlated in the sense of the NE part being closer and moving away, and the SE end being farther and moving towards the sun, all relative to the mean distance and velocity. The bifurcation in distance at the SW end (Fig. 7) at this scale matches the bifurcation in velocity, with the positive velocity H I corresponding to the arm of material seen pulled out of the centre of the SMC in Fig. 7.

Direct evidence that the most distance Cepheids at the SW end have the most negative velocities is provided by the heliocentric mean velocities measured for two SMC Cepheids by

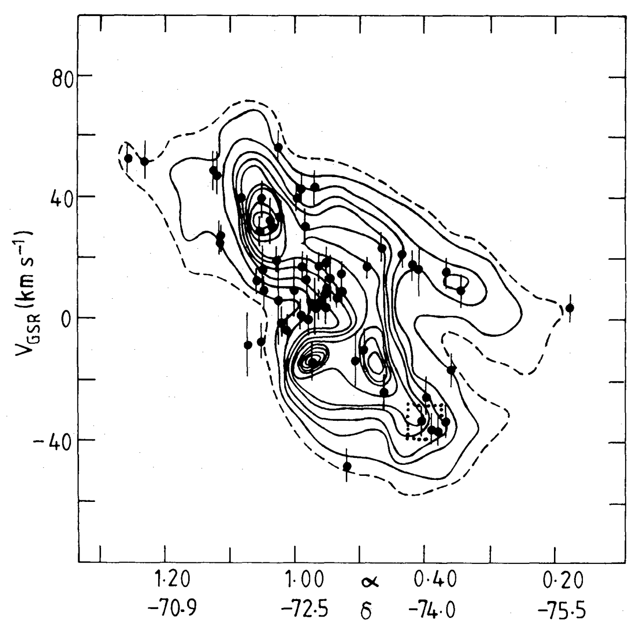

Figure 14. H I velocity profiles along the SMC major axis, abstracted from Mathewson & Ford (1984). The Fig. 7 Cepheid PLC distance moduli are overlaid, suggesting a high degree of negative velocity–distance correlation. Note especially the velocity and distance bifurcation at the SW end. The square denotes the velocity of the two Cepheids for which high-accuracy mean velocities are available. Their negative velocity agrees excellently with their inferred location in the far arm.

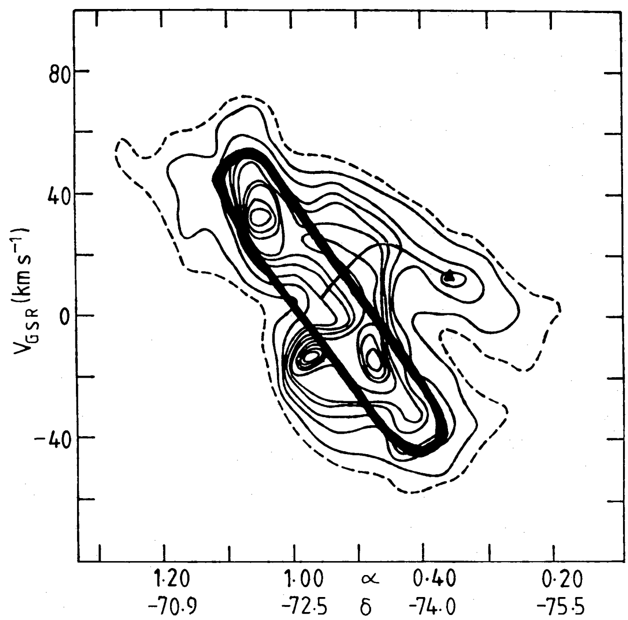

Figure 15. As Fig. 14 abstracted from Mathewson & Ford (1984), but including a sketch of our differing interpretation, which sees the SMC as primarily one body, although extremely spread in distance and velocity from NE to SW. A streamer of material apparently emerging from the centre occurs at a relatively positive velocity in the SW.

CCSF: 126.1±1.8 and 125.5±1.5 km s^{-1} for HV 1365 and 1338, respectively. Their observed mean V_{gsr} (open square in Fig. 14) thus agrees well with that inferred independently by their distance and the velocity–distance correlation. Mathewson & Ford conclude that the SMC is divided into a nearer, low-velocity component (the SMCR) and a farther, high-velocity component (the MMC). Our conclusion from the Cepheid data interprets the velocity picture as sketched in Fig. 15. The SMC has a large velocity gradient (~ -30 km s^{-1} deg^{-1}) from NE to SW, superimposed on which is a disturbance, due to the LMC perhaps, causing an arm of material to be located closer to us in the SW, yet at more positive velocity.

Our picture agrees better with the Cloud orbital modelling of Lin & Lynden-Bell (1982), in the sense that the more distant material has more negative velocity for the reason that it trails in orbit behind the LMC, which is now near perigalacticon. We find good agreement, too, with the Cepheid velocities of Wallerstein (1984), in the sense that they, together with our Cepheid relative distances and two Cepheid means velocities, confirm the inverse correlation of velocity and distance. On the other hand, it is not clear that the interstellar absorption component velocities from Feast, Thackeray & Wesselink (1960) and from Ardeberg & Maurice (1977), cited by Mathewson & Ford, are incompatible with the general trend we find of decreasing velocity at increasing distance, which is contrary to the sense adopted by Mathewson & Ford.

7 Conclusions

Numerical solutions for the observed PL and PLC relations in the Clouds are presented in Tables 1 and 2, which yield the geometrical views of the Clouds in Figs 6 and 7. Expressed in ξ, η coordinates the Clouds have inclinations (mag/deg)

$\nabla\xi = -0.0164 \quad \nabla\eta = -0.0126 \quad$ (LMC)

$\nabla\xi = -0.0861 \quad \nabla\eta = -0.0540 \quad$ (SMC) with respect to the bar centres

$\xi = -418 \qquad \eta = -3114 \qquad \text{(LMC)}$

$\xi = -422 \qquad \eta = -929 \qquad \text{(SMC)}.$

From the Cepheid colours and theory, the Cepheid metallicities in the Clouds are deficient by factors of approximately

1.4–1.6 (LMC)

3.1–3.4 (SMC).

The distance moduli of the Clouds determined using all available luminosity laws (PLC in different colours and PL) depend on ΔZ:

$$\mu_{\mathrm{LMC}} = 18.696 - 6.630\,|\Delta Z| - 317.0\,(\Delta Z)^2$$

$$\mu_{\mathrm{SMC}} = 19.333 - 21.83\,|\Delta Z| - 151.8\,(\Delta Z)^2.$$

Adopting the 'standard' Cloud abundances ($D_{\mathrm{LMC}}=1.4$, $D_{\mathrm{SMC}}=4.0$, $\Delta Y = 2.8\,\Delta Z$) gives

$$\mu_{\mathrm{LMC}} = 18.65 \pm 0.07$$

$$\mu_{\mathrm{SMC}} = 18.97 \pm 0.07.$$

The metal-normal PLC relation is

$$M_V^\circ = -3.53 \log P + 2.13\,\langle B\rangle - \langle V\rangle_0 - 2.25$$

$$(-3.52 \log P + 2.11\,\overline{B-V^\circ} - 2.31).$$

The coefficients for a metal-poor Cepheid would differ as given in Table B1.

The PL relation is [assuming $(m-M)_{\mathrm{M45}} = 5.57$ mag as above]

$$M_V^\circ = -2.78 \log P - 1.41.$$

The Cepheid photometry and radial velocities (in preparation) agree well with published H I velocity data and theoretical modelling of the Magellanic Clouds' orbit, if the more negative velocity material is interpreted to lie at greater distance than the more positive velocity material.

Acknowledgments

We gratefully acknowledge useful discussions with M. W. Feast and C. D. Laney, and helpful correspondence from R. L. Kurucz and R. B. Stothers. We thank M. W. Feast for permission to cite his Cepheid velocities in advance of publication and J. E. Westerhuys for drafting help.

References

Ardeberg, A. & Maurice, E., 1977. *Astr. Astrophys. Suppl.*, **30**, 261.
Ardeberg, A. & Maurice, E., 1979. *Astr. Astrophys.*, **77**, 277.
Azzopardi, M., 1981a. *PhD thesis*, University of Toulouse.
Azzopardi, M., 1981b. In: *The Most Massive Stars*, p. 227, ESO Workshop.
Bajaja, E. & Loiseau, N., 1982. *Astr. Astrophys. Suppl.*, **48**, 71.
Balona, L. A., 1983. In: *Statistical Methods in Astronomy*, p. 187.
Balona, L. A. & Shobbrook, R. R., 1984. *Mon. Not. R. astr. Soc.*, **211**, 375.
Becker, S. A., Iben, I., Jr & Tuggle, R. S., 1977. *Astrophys. J.*, **218**, 633.
Bell, R. A. & Gustafsson, B., 1978. *Astr. Astrophys. Suppl.*, **24**, 299.
Caldwell, J. A. R., 1983. *Observatory*, **103**, 244.
Caldwell, J. A. R. & Coulson, I. M., 1984. *Sth. Afr. astr. Obs. Circ.*, **8**, 1. (see also **9** erratum).

Caldwell, J. A. R. & Coulson, I. M., 1985. *Mon. Not. R. astr. Soc.,* **212,** 879.
Carson, T. R. & Stothers, R. B., 1984. *Astrophys. J.,* **281,** 811.
Coulson, I. M. & Caldwell, J. A. R., 1985. *Mon. Not. R. astr. Soc.,* **216,** 671.
Coulson, I. M., Caldwell, J. A. R. & Gieren, W. P., 1985a. *Astrophys. J. Suppl.,* **57,** 595.
Coulson, I. M., Caldwell, J. A. R. & Gieren, W. P., 1985b. *Astrophys. J.,* in press.
Davies, R. D., Elliott, K. H. & Meaburn, J., 1976. *Mem. R. astr. Soc.,* **81,** 89.
Dean, J. F., Warren, P. R. & Cousins, A. W. J., 1978. *Mon. Not. R. astr. Soc.,* **183,** 569.
de Vaucouleurs, G., 1955. *Astr. J.,* **60,** 126 & 219.
de Vaucouleurs, G., 1980. *Publs astr. Soc. Pacif.,* **92,** 576.
de Vaucouleurs, G. & Freeman, K. C., 1972. *Vistas Astr.,* **14,** 163.
Dennefeld, M. & Stasinska, G., 1983. *Astr. Astrophys.,* **118,** 234.
Dufour, R. J., 1984. *IAU Symp.,* **108,** 353.
Feast, M. W., 1984. *IAU Symp.,* **108,** 157.
Feast, M. W., 1985. In: *Cepheids: Theory and Observations, IAU Colloq.,* **82,** 157.
Feast, M. W. & Whitelock, P. A., 1984. *Observatory,* **104,** 193.
Feast, M. W., Thackeray, A. D. & Wesselink, A. J., 1960. *Mon. Not. R. astr. Soc.,* **121,** 337.
Fernie, J. D. & McGonegal, R., 1983. *Astrophys. J.,* **275,** 732.
Florsch, A., Marcout, J. & Fleck, E., 1981. *Astr. Astrophys.,* **96,** 158.
Gascoigne, S. C. B. & Shobbrook, R. R., 1978. *Proc. astr. Soc. Australia,* **3,** 285.
Hodge, P. W., 1972. *Publ. astr. Soc. Pacific,* **84,** 365.
Hodge, P. W., 1974. *Publ. astr. Soc. Pacific,* **86,** 263.
Hodge, P. W. & Wright, F. W., 1967. *The Large Magellanic Cloud,* Smithsonian Press, Washington D.C.
Hodge, P. W. & Wright, F. W., 1977. *The Small Magellanic Cloud,* University of Washington Press, Seattle.
Iben, I., Jr & Tuggle, R. S., 1975. *Astrophys. J.,* **197,** 39.
Iben, I., Jr & Renzini, A., 1984. *Phys. Rep.,* **105,** 329.
Lequeux, J., Peimbert, M., Rayo, J. F., Serrano, A. & Torres-Peimbert, S., 1979. *Astr. Astrophys.,* **80,** 155.
Lin, D. N. C. & Lynden-Bell, D., 1982. *Mon. Not. R. astr. Soc.,* **198,** 707.
McGee, R. X. & Newton, L. M., 1981. *Proc. astr. Soc. Australia,* **4,** 189.
McGregor, P. J. & Hyland, A. R., 1984. *Astrophys. J.,* **277,** 149.
Martin, W. L. & Warren, P. R., 1979. *Sth. Afr. Astr. Obs. Circ.,* **4,** 98.
Martin, W. L., Warren, P. R. & Feast, M. W., 1979. *Mon. Not. R. astr. Soc.,* **188,** 139.
Mathewson, D. S. & Ford, V. L., 1984. *IAU Symp.,* **108,** 125.
Nandy, K., 1984. *IAU Symp.,* **108,** 341.
Pel, J. W., 1984. In: *Proc. Second Asian-Pacific Regional Meeting on Astronomy,* p. 411.
Pel, J. W., 1985. In: *Cepheids: Theory and Observations, IAU Colloq. 82,* p. 1.
Prevot, M. L., Lequeux, J., Maurice, E., Prevot, L. & Rocca-Volmerange, B., 1984. *Astr. Astrophys.,* **132,** 389.
Rohlfs, K., Kreitschmann, J., Siegman, B. C. & Feitzinger, J. V., 1984. *Astr. Astrophys.,* **137,** 343.
Schaltenbrand, R. & Tammann, G. A., 1971. *Astr. Astrophys. Suppl.,* **4,** 265.
Schmidt-Kaler, T., 1982. *Landolt-Börnstein VI 2b,* eds Schaifers, K. & Voigt, H. H., Springer-Verlag, Berlin.
Stift, M. J., 1982. *Astr. Astrophys.,* **112,** 149.
Stothers, R. B., 1983. *Astrophys. J.,* **274,** 20.
Turner, D. G., 1984. *Publ. astr. Soc. Pacific,* **96,** 422.
Turner, D. G. & Evans, N. R., 1984. *Astrophys. J.,* **283,** 254.
van Genderen, A. M., 1981. *Astr. Astrophys.,* **101,** 289.
van Genderen, A. M., 1983. *Astr. Astrophys.,* **124,** 223.
Walker, A. R., 1985. *Mon. Not. R. astr. Soc.,* **213,** 889.
Wallerstein, G., 1984. *Astr. J.,* **89,** 1705.
Wesselink, A. J., 1959. *Mon. Not. R. astr. Soc.,* **119,** 576.

Appendix A. Details of method of solutions

Following Balona (1983) our statistical model is

$$z=\alpha x+\beta y+\gamma$$

where

$$z=V-R\cdot E$$

$x = \log P$

$y = C - f \cdot E$

and

$E = E(B-V)$

$C = B-V$ or $V-I$

$f = 1$ if $C = B-V$

$= \mathrm{E}(V-I)/E(B-V)$ if $C = V-I$

We assume V is measured with error σ_V, C with error σ_C, E with error σ_E, and $\log P$ with negligible error. σ_V, σ_C and σ_E are assumed to be uncorrelated. A normal multilinear least-squares problem results if $\sigma_C = \sigma_E = 0$ and all scatter is assumed to reside in V due to σ_V and any line-of-sight dispersion. A normal maximum-likelihood problem results if $\sigma_C \neq 0$, and a slightly more complicated solution is required if $\sigma_E \neq 0$ because of the resulting correlated error $\sigma_{yz} \neq 0$.

We observe values z_i, x_i, y_i for each Cepheid 'i' (more generally z_i can be corrected for the Cloud inclination by iteration), and have estimates of σ_V^i, σ_C^i and σ_E^i. Then our model becomes

$$z_i + \sigma_V^i + R\sigma_E^i = \alpha x_i + \beta(y_i + \sigma_C^i + f\sigma_E^i) + \gamma.$$

Following Balona (1983) we obtain simultaneous equations for α, β and γ:

$$\Sigma x_i z_i = \alpha \Sigma x_i^2 + \beta \Sigma x_i y_i + \gamma \Sigma x_i$$

$$\Sigma y_i z_i - NRf\sigma_E^2 = \alpha \Sigma x_i y_i + \beta(\Sigma y_i^2 - N\sigma_C^2 - Nf^2\sigma_E^2) + \gamma \Sigma y_i$$

$$\Sigma z_i = \alpha \Sigma x_i + \beta \Sigma y_i + N\gamma,$$

corresponding to the unweighted case $\sigma_C^i \equiv \sigma_C$ and $\sigma_E^i \equiv \sigma_E$.

Since the brighter Cepheids are typically much better observed than the fainter ones, we weight each star by σ_F^i, where

$$F_i = V_{\mathrm{obs}}^i - V_{\mathrm{calc}}^i$$

$$(\sigma_F^i)^2 = (\sigma_V^i)^2 + \beta^2(\sigma_C^i)^2 + (R - f\beta)^2(\sigma_E^i)^2.$$

Individual weights are introduced in the preceding system of three equations by means of the following substitutions:

$$\Sigma() \to \Sigma()/(\sigma_F^i)^2, \qquad \sigma^2 \to \Sigma(\sigma^i)^2/(\sigma_F^i)^2 \qquad \text{and } N \to \Sigma 1/(\sigma_F^i)^2.$$

R and f are also treated as being variable, R_i and f_i, depending on the Cepheid mean colour. The solution by standard methods gives the three unknowns α, β and γ from the three equations. Since the weighting depends on β, the solution is iterated (quickly) to the final β.

The PL and PC solutions are straightforward weighted least-squares solutions with $\sigma_{\mathrm{PL}}^i = \sigma_z^i$ and $\sigma_{\mathrm{PC}}^i = \sigma_y^i$. The universal PLC and PL solutions simply add an extra variable T, equal to 0 for the LMC and 1 for the SMC, yielding an extra equation and one more unknown δ, the differential distance modulus between the two Cloud centres. In addition, z_i must be corrected for $\Delta\alpha$, $\Delta\beta$ and $\Delta\gamma$ between the two Clouds in this case (Appendix B).

Full expressions for σ_α, σ_β and σ_γ were developed for the maximum-likelihood case. In general $\sigma_\alpha^{\mathrm{ML}} > \sigma_\alpha^{\mathrm{LS}}$, $\sigma_\beta^{\mathrm{ML}} > \sigma_\beta^{\mathrm{LS}}$ and $\sigma_\gamma^{\mathrm{ML}} < \sigma_\gamma^{\mathrm{LS}}$, due to the reapportionment of the errors in the maximum-likelihood hypothesis. Since $\sigma_\gamma^{\mathrm{ML}}$ can be unrealistically small if the colour and reddening errors are overestimated, $\sigma_\alpha^{\mathrm{ML}}$, $\sigma_\beta^{\mathrm{ML}}$ and $\sigma_\gamma^{\mathrm{LS}}$ were adopted for the coefficients α, β and γ.

$$\sigma^2_{\mathrm{VTOT}}=(\Sigma z_i^2-\alpha\Sigma x_i z_i-\beta\Sigma y_i z_i-\gamma\Sigma z_i)/(N-3)-R(R-f\beta)\sigma_E^2$$

gives in the unweighted limit the total spread in V. Any spread in V not attributable to observational error, σ_V, was assumed to be line-of-sight scatter:

$$\sigma^2_{\mathrm{VLOS}}=\sigma^2_{\mathrm{VTOT}}-\sigma_V^2$$

The solutions yield the multilinear least-squares results for the coefficients in the two limits when all the scatter is attributed to $V°$ or to $C°$. The solutions yield coefficients midway between the two limits when $\sigma_V^\circ/\sigma_C^\circ$ is set equal to ratio of the PL-relation width to the PC-relation width, in accordance with expectation. Allowing for correlation of the errors in $V°$ and $C°$ due to $\sigma_E\neq 0$ produces a small additional shift in the solutions towards the least-squares-in-V-limit.

Observational errors σ_V^i, σ_C^i and σ_E^i ($\geqslant$0.010 mag) were adopted for all Cepheids. The reddening errors came from CC2 for the individual reddening determinations, but were adopted to be the intrinsic standard deviation of the observed reddenings in cases where the average Cepheid reddening value was assumed (Section 1). These standard deviations are 0.028 mag for the LMC Cepheids in the solution and 0.021 mag for the SMC. For the LMC the magnitude and colour errors were taken from an analysis of MWF Table 2, from which it was calculated that σ_V=0.025 mag and σ_C=0.030 mag approximate the s.e.m. of the Cepheid results there; following MWF no weighting was attempted. The MWF analysis took a straight mean of the Cepheid mean colours from different sources, with no attempt to combine the actual data from all sources to improve the phase coverage. Thus errors are expected to be rather larger than in the SMC

Table A1. Cepheids treated exceptionally.

LMC Cepheid	Log P	Reason	SMC Cepheid	Log P	Reason
HV 883	2.127	1	HV 1956	2.317	1
2447	2.077	1	821	2.106	1
2883	2.033	1	MKg	1.593	2
2749	1.364	2	HV 1636	1.514	5
2301	0.978	6	10357	1.506	2
12869	0.786	3	1369	1.490	6
12765	0.668	3	1451	1.478	2
2353	0.624	3	1501	1.438	2
			1552	1.345	2
			1543	1.311	2
			1482	1.199	2
			1560	1.191	2
			1442	1.184	2
			1579	1.164	2
			1438	1.135	2
			1630	1.057	2
			6320	1.004	4
			1484	0.954	6
			1437	0.923	2

Reasons
1, Period too long. 2, Reddening in doubt. 3, Probable overtone. 4, Location incompatible with simplified geometry. 5, Blue companion. 6, Peculiar (*cf.* text).

analysis (CC1) because of phase gaps in the material and because of weighting the poorer material equally with the better. The weighted mean values for the errors in the various solutions fall in these ranges:

	σ_V	σ_C	σ_{EBV}	σ_{EVI}
LMC	0.025	0.030–032	0.023–028	0.033–037
SMC	0.011–014	0.011–018	0.020–024	0.026–030.

A number of Cepheids were omitted entirely from the solutions or else treated in some exceptional manner, as discussed here. Table A1 lists the Cepheids treated differently and why. Five Cepheids with $P>100$ d were given zero weight based on the empirical finding that Cepheids of such extreme period are likely to be anomalous in all galaxies, and based on theoretical considerations (Carson & Stothers 1984). Fourteen Cepheids located within a zone of apparently high obscuration near dark nebulae and lacking individual reddening determinations, were given zero weight. Three Cepheids were assumed to be overtone pulsators and their theoretical fundamental period was adopted following MWF. R Hyi (HV 6320) was too far preceding the SMC to be compatible with a planar model for the Cloud, and was thus omitted from the magnitude regressions although included in the PC law. HV 1636 was assumed to have B2V companion following CC2, and an average Cepheid reddening. Of particular interest are the remaining 'deviants', which were given no weight and which deserve further study: HV 2301 (MWF), HV 1369 (extremely deviant light curve shape and low blue amplitude in CC1, see also van Genderen 1981) and HV 1484 in the SMC which appears to be a very similar case to HV 2301 in the LMC.

The 13 Cepheids in the dusty core zone of the SMC were excluded from the solution because of lacking individual reddening values where the reddening is likely to be very scattered. However, they enable a rough mean $E(B-V)$ to be calculated for this central SMC area of approximately 0.24 ± 0.06 mag, on the assumption that their mean distance modulus must coincide with the inclined plane model inferred from all the other Cepheids.

Appendix B: Abundance effects on the PLC

If Cepheids in the Galaxy obey $z=\alpha x+\beta y+\gamma$ (Appendix A), then in a metal-poor galaxy they will obey $z=(\alpha+\Delta\alpha)x+(\beta+\Delta\beta)y+(\gamma+\Delta\gamma)$, where $\Delta\alpha$, $\Delta\beta$ and $\Delta\gamma$ are to be obtained theoretically as a function of metals and helium deficiency. Iben & Tuggle's (1975) equation (11) gives the P-L-T-α_{ML}-β_{ML} relation, where α_{ML} and β_{ML} are the coefficients of the Cepheid mass–luminosity law. Becker, Iben & Tuggle (1977) equations (8) and (9) evaluate α_{ML} and β_{ML} in terms of ΔZ and ΔY, yielding an abundance-dependent theoretical PLT relation. Theoretical bolometric corrections and $B-V$ colours from Bell & Gustafsson (1978) and $V-I$ colours from Kurucz (personal communication) then yield an abundance-dependent theoretical PL$_V C$ relation, where $B-V$=function ($\log T$, $\log g$, ΔZ) introduces a further abundance effect.

The $\log P$–M_V–colour relation is not linear. Iben & Tuggle (1975) and Iben & Renzini (1984) have linearized it to a form $z=\alpha x+\beta y+\gamma$ by expansion in the vicinity of one point, whereas van Genderen (1983) has expanded it at several periods, obtaining a different PLC at each. Our approach has been to Taylor-expand the non-linear PLC relation along the Cepheids ridge line. An expression is thus obtained for any metal abundance:

$$M_V^\circ=\alpha\log P+\{\beta_0+\beta_1(\log P-1.25)\}\,\mathrm{colour}^\circ+\gamma,$$

which numerically agrees well with the full non-linear PLC expression everywhere in the instability strip, rather than near just one of a few loci.

We confirm van Genderen's (1983) point that the colour term β is theoretically not a constant

Table B1. Theoretical abundance effect on PLC.

$B-V$	$\Delta\alpha$	$\Delta\beta$	$\Delta\gamma$	β_1	$(\Delta\alpha)$	$(\Delta\gamma)$
$D=1$	0	0	0	1140	0	0
1.4	−25	44	169	1110	17	118
2	−48	88	322	1090	32	226
4	−91	157	559	1060	47	393
8	−125	196	706	1050	50	494
1.4y	−42	46	150	1120	−4	104
2y	−82	95	295	1100	−7	204
4y	−146	170	527	1070	−14	367
8y	−197	216	675	1060	−27	469
$V-I$	$\Delta\alpha$	$\Delta\beta$	$\Delta\gamma$	β_1	$(\Delta\alpha)$	$(\Delta\gamma)$
$D=1$	0	0	0	1080	0	0
1.4	−17	39	88	1060	5	61
2	−35	78	163	1030	7	113
4	−69	140	264	1000	0	181
8	−99	175	305	980	−16	206
1.4y	−34	41	69	1060	−16	47
2y	−69	85	135	1040	−33	91
4y	−125	153	229	1000	−61	153
8y	−170	195	270	990	−92	177

All units 0.001.

with log P, although the range of β he obtains is small (~10 per cent) over the log P range of interest (0.5–2.0). We obtain here a larger theoretical period dependence for β (~30 per cent) for the simple reason of rejecting the linear bolometric correction-(log T) regression of previous workers as being an exceedingly poor fit. A quadratic BC–(log T) relation fits the models much better, which implies that β must increase yet more strongly with increasing log P.

Table B1 gives the theoretical abundance effect of the coefficients α, β and γ obtained by the analysis just sketched. In the Table, D is the abundance deficiency as defined in Section 2 and Δ refers to the change in the coefficients in the sense (deficient–normal). The first three columns give $\Delta\alpha$, $\Delta\beta$ and $\Delta\gamma$ where an average for β has been used (at log P=1.25) and $\beta_1(=\partial\beta/\partial \log P)$ has been ignored; these coefficients were used for the standard solutions, which assume that β is a constant with log P. Alternative solutions (Section 4) considered the possibility indicated by theory that β is an increasing function of log P, with slope β_1. In this case the appropriate abundance shifts are calculated to be $(\Delta\alpha)$, $\Delta\beta$ and $(\Delta\gamma)$.

Iben & Renzini (1984) have reiterated that the coefficients of the PL relation are to a very good approximation independent of composition, despite the likely composition dependence of the strip edges (Pel 1984).